THE JOURNAL OF BIOLOGICAL CHEMISTRY VOL. 287, NO. 10, pp. 7324–7334, March 2, 2012

Role of Runt-related Transcription Factor 3 (*RUNX3*) in Transcription Regulation of Natural Cytotoxicity Receptor 1 (*NCR1/NKp46*), an Activating Natural Killer (NK) Cell Receptor*[S]

Received for publication, September 22, 2011, and in revised form, January 5, 2012 Published, JBC Papers in Press, January 17, 2012, DOI 10.1074/jbc.M111.306936

C. Benjamin Lai and Dixie L. Mager[1]

From the Terry Fox Laboratory, British Columbia Cancer Agency and Department of Medical Genetics, University of British Columbia, Vancouver, British Columbia V5Z1L3, Canada

Background: The expression of the activating receptor NKp46/NCR1 is highly restricted to NK cells.
Results: RUNX proteins bind identified cis-regulatory element and affect NCR1 expression.
Conclusion: NCR1 is regulated by two key proximal cis-regulatory elements and by RUNX factors.
Significance: Mapping regulatory components of NCR1 will contribute to a deeper understanding of NK biology.

Natural cytotoxicity receptor 1 (NCR1), also known as NKp46, is a natural killer (NK) lymphocyte-activating receptor. It is involved in major aspects of NK immune function and shows a high degree of lineage specificity in blood and bone marrow. The nature of its NK-restricted expression is not well understood. In this study, we confirm that human NCR1 NK-specific expression is achieved at the mRNA level. We found two key cis-regulatory elements in the immediate vicinity upstream of the gene. One element acts as an essential promoter, whereas the other acts as a tissue-dependent enhancer/repressor. This latter regulatory element contains a runt related-transcription factor (RUNX) recognition motif that preferentially binds RUNX3. Interfering with RUNX proteins using a dominant negative form results in decreased *Ncr1* expression. RUNX3 overexpression had the opposite effect. These findings shed light on the role of RUNX3 in the control of an important NK-activating receptor.

Natural killer (NK)[2] cells are large granular lymphocytes that have antiviral, anticancer, and immunoregulatory functions (1). Recent findings suggest that they possess memory reminiscent of adaptive T and B cells (2). However, they have long been considered as part of the innate branch due to their reliance on germ-line encoded receptors. The large number of NK receptors can be categorized into inhibiting, typified by NKG2A, the Ly49, and the killer immunoglobulin-like receptors, and activating, including NKG2D and the natural cytotoxicity receptors (3).

NKp46 is an activating receptor encoded by natural cytotoxicity receptor 1 (*NCR1*). It is a type 1 transmembrane protein containing two immunoglobulin-like domains, initially identified via a redirected killing assay screen (4). Monoclonal antibody-mediated cross-linking of NKp46 induces calcium mobilization, cytolytic activity, as well as interferon γ (IFNG) release. Only one natural ligand has been discovered for NKp46 so far: the viral hemagglutinin (5). However, NCR1/NKp46 is postulated to have unknown tumor ligands that can participate in tumor immunoediting (6). The emerging role of NKp46 is highlighted in studies on mice deficient for *Ncr1*. These knock-out mice are unable to fight influenza infection, unable to control a specific experimental lymphoma model, and are more protected from development of type 1 diabetes (7–9).

NCR1 is unique among NK surface receptors. Unlike some of the other receptors, *NCR1* is highly conserved in mammals (10–12). Perhaps most interestingly, NCR1 and NCR3 are the only NK receptors that show relatively high expression specificity (13). Recent studies indicate that NKp46 also marks mouse gut RORC+IL22+ innate immune cells and human tonsil CD127+RORC+ lymphoid tissue inducer-like cells (14, 15), calling into question the specificity of the receptor. However, at least in the bone marrow and blood, NKp46 acts as a *bona fide* NK marker (16).

The expression pattern of NCR1 alludes to specific transcriptional control. Thus, studying its regulation provides an opportunity to identify important transcription factors of the natural killer lineage. Furthermore, the *NCR1* promoter is on the verge of becoming a widely used and efficacious tool to study the biology of conventional NK cells. Already, one study has used it to ablate NK cells *in vivo*, whereas another used it to create an NK-specific *Stat5*-deficient mouse (16, 17). However, the mechanism behind its precise control has so far gone largely unaddressed. Here we focus on the proximal upstream region of the human *NCR1* gene. We identify two cis-regulatory ele-

* This work was supported by a grant from the Canadian Institutes of Health Research with core support provided by the British Columbia Cancer Agency.
[S] This article contains supplemental Table S1 and Figs. S1–S3.
[1] To whom correspondence should be addressed: Terry Fox Laboratory, BC Cancer Agency, 675 West 10th Ave., Vancouver, British Columbia V5Z1L3, Canada. Tel.: 604-675-8139; Fax: 604-877-0712; E-mail: dmager@bccrc.ca.
[2] The abbreviations used are: NK, natural killer; NCR, natural cytotoxicity receptor; IFNG, interferon γ; RUNX, runt-related transcription factor; hRUNX, human RUNX; RORC, retinoic acid related orphan receptor c; PBMC, peripheral blood mononuclear cells; APC, allophycocyanin; PE, phycoerythrin; ACTB, β actin; ETS, E-twenty six family; dn-RUNX, dominant negative RUNX; H3K4me3, histone 3 lysine 4 trimethylation; H3K27me3, histone 3 lysine 27 trimethylation; γc, common γ chain; Bis-Tris, 2-(bis-(2-hydroxyethyl)amino)-2-(hydroxymethyl)propane-1,3-diol; NKP, NK progenitor.

ments in this region and describe a role of runt-related transcription factor (RUNX) proteins, especially RUNX3, in regulating *NCR1* expression.

EXPERIMENTAL PROCEDURES

PBMC Flow Cytometry—Peripheral blood was obtained from healthy donors, and peripheral blood mononuclear cells (PBMC) were isolated by density centrifugation on Ficoll PLUS (StemCell Technologies). PBMC were then washed with PBS containing 5% human serum (Sigma H4522), and Fc receptors were blocked using human Fc receptor blocking reagent (Miltenyi). Next, the cells were stained using monoclonal antibodies: CD335/NKp46-APC (Miltenyi 130-092-609), CD3-FITC (BD Biosciences 555332), CD56-PE (StemCell Technologies 10526), CD14-FITC (StemCell Technologies 10406), CD15-FITC (BD Biosciences 555401), CD19-PE (Beckman Coulter IM1285U), and CD33-PE (BD Biosciences 347787). Isotype control antibodies were: IgG_1-APC (BD Biosciences 555751), IgG_1-FITC (StemCell Technologies 10310), IgG_1-PE (StemCell Technologies 10311), IgG_{2b}-FITC (BD Biosciences 555742), IgG_{2b}-PE (BD Biosciences 555743), and IgM-FITC (BD Biosciences 555583). Lastly, propidium iodide was added to 5 μg/ml. Four-color analysis was carried out using FACSCalibur.

Cell Culture—NK92, a human NK cell line (18), was cultured in minimum essential medium Eagle's with Earle's salts and nonessential amino acids, supplemented with 12.5% (v/v) fetal bovine serum, 12.5% (v/v) horse serum, 2 mM L-glutamine, 100 μM 2-mercaptoethanol, 100 units/ml IL-2 (PeproTech). KY-2 and LNK (both mouse NK cell lines) were cultured in RPMI 1640 medium supplemented with 10% (v/v) fetal bovine serum, 2 mM L-glutamine, and 50 μM 2-mercaptoethanol. LNK and KY-2 used 1000 units/ml and 200 units/ml of IL-2, respectively. U2OS (human osteosarcoma), K562 (human erythroleukemia), LoVo (human colorectal adenocarcinoma), HEK-293 (human embryonic kidney), and NIH-3T3 (mouse embryonic fibroblast) cells were cultured in Dulbecco's modified Eagle's medium supplemented with 10% (v/v) fetal bovine serum (fetal calf serum for NIH-3T3). IM-9 (human B-lymphoblastoid), Jurkat (human T-lymphocyte), THP-1 (human acute monocytic leukemia), and HL-60 (human acute promyelocytic leukemia) cell lines were cultured in RPMI 1640 medium supplemented with 10% (v/v) fetal bovine serum. Mouse NK cells were isolated from spleen of *Runx3*-deficient (19) and wild type mice by negative selection (R&D MagCollect mouse NK cell isolation kit, MAGM210) and cultured for 7 days in RPMI 1640 medium containing 10% (v/v) fetal calf serum, 2 mM L-glutamine, 1% sodium pyruvate, 1% nonessential amino acids, 50 μM 2-mercaptoethanol, and 1000 units/ml IL2 (Biological Industries, Beit-Haemek, Israel, 30-T209B). All cultures were supplemented with 100 units/ml penicillin, 100 units/ml streptomycin.

RT-PCR and Real-time PCR—Total RNA from cells were collected using RNeasy mini kit and QIAshredder homogenizer (Qiagen). RNA samples were treated with Turbo DNase (Ambion) before cDNA conversion using SuperScript III and random primers (Invitrogen). Primers used for PCR are listed in supplemental Table S1. Real-time PCR was done using the 7500 Fast real-time PCR system (Applied Biosystems). Relative expression was determined using the $2^{-\Delta\Delta CT}$ method. Threshold cycles were normalized to *Actb*.

Generation of Luciferase Reporter Constructs—Promoter fragments were generated by PCR using forward primers with KpnI site inserted at the 5′ end and reverse primers with NheI site inserted at the 5′ end. PCR products were digested with KpnI/NheI (New England Biolabs) and cloned into pLG4.10 (pGL4B) firefly luciferase promoter vector (Promega). RUNX mutations were introduced into the 5′-270 construct using the QuikChange Lightning site-directed mutagenesis kit (Stratagene). For all primer sequences, see supplemental Table S1.

Transient Transfection and Luciferase Assays—NK92 and U2OS cells were transiently transfected with Lipofectamine LTX with PLUS reagent (Invitrogen) according to manufacturer's instructions. Briefly, 1.0×10^5 NK92 cells and 5.0×10^5 U2OS cells were seeded into 500 μl of growth medium without penicillin/streptomycin in 24-well plates for 24 h at 37 °C. For each well, 100 μl of LTX transfection medium was prepared: 2 μl of LTX reagent, 1 μg of vector, 0.1 μg of pRL-TK, 1 μl of PLUS, topped up with medium without serum. The mix was incubated for 30 min prior to addition to wells. Cells were incubated at 37 °C for 24 h before assaying.

Luciferase activity was assayed using the Dual-Luciferase reporter assay system (Promega) according to the manufacturer's instructions. Firefly luciferase activity was normalized relative to *Renilla* luciferase activity for each transfection and calculated as -fold increase over pGL4.10-BASIC (pGL4B).

Western Blot—Nuclear extraction was performed as described before (20). Protein concentration was determined using the NanoDrop ND-1000 (Thermo Scientific). NuPAGE Novex 4–12% Bis-Tris gels (Invitrogen) were used to resolve the protein sample in MOPS SDS running buffer (Invitrogen). Proteins were transferred onto an Immobilon-P PVDF membrane (Millipore) in transfer buffer (25 mM Tris, 192 mM glycine, 10% methanol, 0.1% SDS). The membrane was blocked for 1 h with blocking solution: 5% (w/v) skim milk reconstituted with TBST buffer (20 mM Tris, 150 mM NaCl, 0.1% Tween 20). Primary antibody was then added at 1:3000 anti-RUNX3 (Abcam ab11905) and 1:3000 anti-ACTB (Sigma A2066) overnight at 4 °C with constant agitation. The membrane was washed five times with TBST buffer at room temperature with 5-min intervals. Goat anti-rabbit (Sigma A0545) at 1:10,000 was diluted in TBST buffer with 0.5% (w/v) of skim milk. The membrane was incubated in this secondary antibody solution for 1 h at room temperature under constant agitation. Washes were carried out as above. Protein was detected using SuperSignal (Thermo Scientific) and Kodak BioMax MR film.

EMSA—Wild type and mutated double-stranded probes containing the putative RUNX binding sites were generated by annealing oligomers (oligomers listed in supplemental Table S1). Nuclear extraction, probe labeling, and the gel shift assay were performed as described before (20). Seven μg of protein was used per binding reaction (protein concentration was determined using the NanoDrop ND-1000 (Thermo Scientific)). For supershift experiments, 2.5 μl of anti-RUNX3 (Abcam ab11905) and 2.5 μg of anti-RUNX1 (Abcam ab23980) was used.

Chromatin Immunoprecipitation—ChIP assay was performed as described previously (21) with the following modifications. Formaldehyde cross-linking was done for 15 min at room temperature for cell lines and 10 min for mouse NK cells. Sonication was done using 30-s on, 30-s off cycles (25 cycles for NK92, 30 cycles for U2OS and IM-9, 20 cycles for mouse NK cells). Preclearing and pulldown utilized protein A/G beads (Thermo Scientific). Immunoprecipitation was accomplished with 5 μl or 5 μg of anti-RUNX3 (Abcam ab11905), anti-RUNX1 (Abcam ab23980), anti-histone 3 lysine 4 trimethylation (Millipore CS200580), anti-histone 3 lysine 27 trimethylation (Abcam ab6002), and normal rabbit IgG (Millipore).

Retrovirus Transduction and Fluorescence-assisted Cell Sorting—Control MIGR1, dominant negative RUNX (dn-RUNX) on MIGR1 backbone (HA-NLS-Runt), and human RUNX3 (hRUNX3) cDNA on MIY backbone (MIY-hRUNX3) have been described previously (22, 23). These vectors were transiently transfected into Plat-E (24) using TurboFect *in vitro* reagent (Fermentas) according to the manufacturer's instructions. Forty-eight hours later, viral supernatant was collected and used immediately or stored in −80 °C. The growth medium of KY-2 cells was switched with viral supernatant plus 4 μg/ml Polybrene (Sigma) and 200 units/ml IL-2 (PeproTech). For the MIY-hRUNX3 experiments, the viral supernatant was switched back to growth medium after 24 h. For the dn-RUNX experiments, KY-2 cells were subjected to a second round of infection as above after 24 h. Another 24 h passed for the second round before the KY-2 culture was switched back to growth medium. Two or 4 days after the switch, fluorescence-assisted cell sorting was used to isolate GFP+ or YFP+ cells. Cells were allowed to recover from sorting stress for 24 h in growth medium before RNA collection.

RESULTS

NKp46/NCR1 Expression Specificity Stems from Transcript Level—NKp46/NCR1 is widely accepted as a *bona fide* NK marker at least in blood. There is good evidence for NKp46 specificity at the cell surface in both human and mouse (4, 16). Indeed, in healthy human PBMC, almost all NKp46+ cells also express CD56, but not T, B, or myeloid lineage markers CD3, CD19, CD14, CD15, and CD33 (Fig. 1*A*). However, few have checked whether the expression pattern is reflected at the transcriptional level in human. We addressed this issue by performing semiquantitative RT-PCR on a panel of human cell lines and surveying publicly available microarray data. In accordance with a previous study (25), out of a panel of human cell lines (NK, T, B, monocyte, promyeloblast, erythroid, osteosarcoma, and embryonic kidney), only the NK cell line shows *NCR1* expression (Fig. 1*B*). In primary tissue, as shown by published microarray data, *NCR1* transcripts are also confined to the NK lineage (Fig. 1*C*). These results suggest that the NK-specific expression of NKp46 is transcriptionally controlled and that the cell line, NK92, is a good NK model to further study the mechanism of its regulation.

Human NCR1 Promoter Contains Essential and Enhancing Region—Walzer *et al.* (16) were able to drive NK-specific expression using just 400 bp of noncoding sequence upstream of the human *NCR1* gene, suggesting that all the important

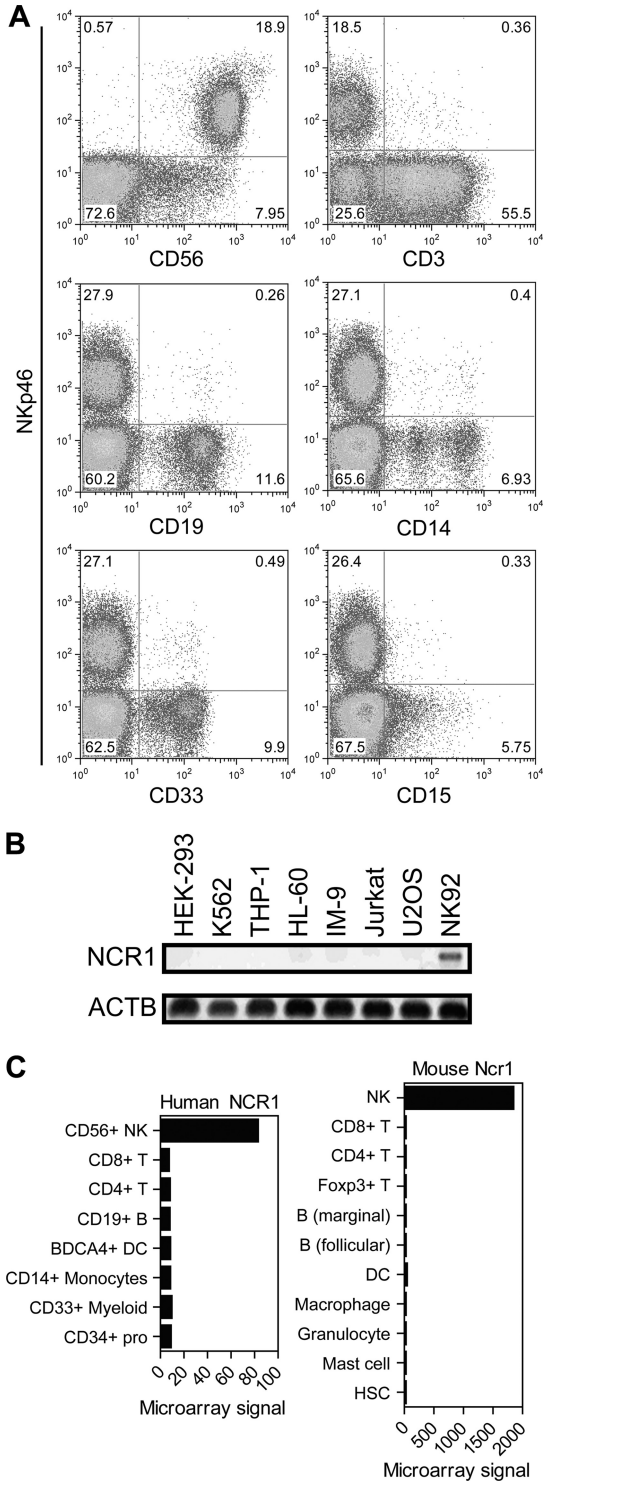

FIGURE 1. **NCR1 transcript is NK-specific.** *A*, phenotypic analysis of healthy human PBMC. Freshly isolated PBMC were stained for NKp46 and other indicated lineage markers. Dot plots show representative data from three independent experiments. *B*, RT-PCR detection of *NCR1* in human cell lines with *ACTB* as internal control. Total RNA from indicated cell lines was used for reverse transcriptase reactions. *C*, microarray of *NCR1* expression. Data were accessed through BioGPS (51). Human data are from GeneAtlas U133A probe set 207860_at (52). Mouse data are from GeneAtlas MOE430 probe set 1422089_at (53). Only relevant hematopoietic cell types are shown. *Pro*, progenitor; *DC*, dendritic cell; *HSC*, hematopoietic stem cell.

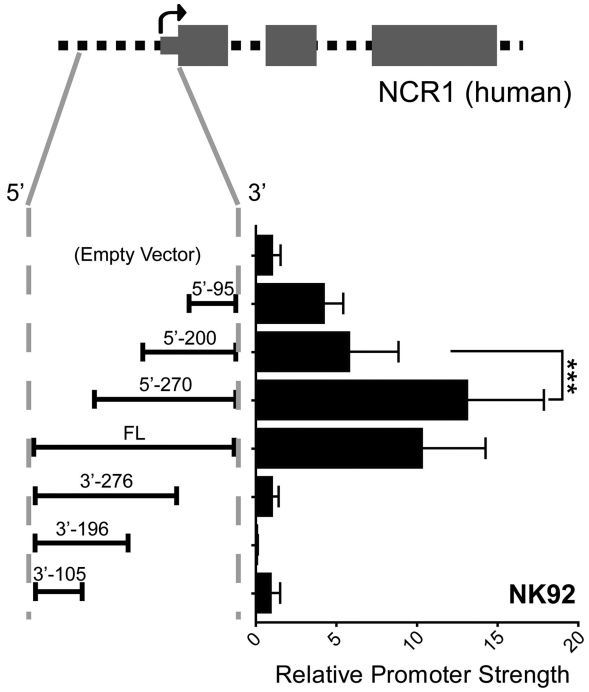

FIGURE 2. **Luciferase reporter assay of *NCR1* promoter in NK92.** A diagram of the promoter and first three exons of *NCR1* is shown at the top. 5′-UTR and coding regions are shown as *thin* and *thick gray boxes*, respectively. The *black arrow* depicts the TSS. Promoter fragments truncated from the 5′ and 3′ ends were cloned into pGL4B and transiently transfected into NK92. Firefly luciferase activity was assayed normalized to co-transfected *Renilla* luciferase activity. Promoter strength is calculated as -fold above pGL4B empty vector. Data shown represent means with standard deviations of more than three experiments. Tests of significance were carried out using analysis of variance followed by Tukey's post test (***, $p < 0.001$).

cis-regulatory elements are immediately upstream of the gene itself. In agreement with this, the level of genomic conservation upstream of the start codon of human NCR1 is limited to ~300 bp (supplemental Fig. S1). To further pinpoint the crucial cis-regulatory elements, we cloned −396 to +1 relative to the ATG into pGL4B (designated FL; Fig. 2). We also made truncation mutants designated with the suffix 5′ or 3′ (depending on the direction of truncation) followed by the size of the remaining promoter. These constructs were transiently transfected into NK92 cells, and luciferase assays were conducted. The 5′-95 construct, corresponding to the region immediately upstream of the ATG, shows appreciable promoter activity (~4-fold above background). This fragment acts as an essential promoter because its removal, as seen in the 3′ truncations, completely abrogates activity. In addition, we observe a significant gain of promoter strength between 5′-200 and 5′-270 constructs (from 6- to 13-fold above background). Thus, there appears to exist an enhancer between −270 and −200. The differences between 5′-95 and 5′-200, or between FL and 5′-270, were not statistically significant. We conclude that there are no major cis-regulatory sequences between −95 to −200 and −270 to −396. These human constructs showed a similar trend in the mouse NK cell line, KY-2, suggesting that the promoter is not species-specific (supplemental Fig. S2).

NCR1 Promoter Contains RUNX Sites, and RUNX Members Are Expressed in NK Cells—To identify the transcription factors that regulate the *NCR1* promoter, we scanned the promoter sequence for transcription factor binding motifs using the Transcription Element Search System (TESS). Curated results containing only mammalian hematopoietic transcription factors are shown in Fig. 3*A*. To narrow down the list, we focused on the essential and enhancing cis-regulatory regions and took two approaches. Firstly, we carried out a semiquantitative RT-PCR screen to check the expression of the predicted transcription factors in NK *versus* other cell types. None of the predicted factors had an expression pattern as specific as *NCR1* (Fig. 3*B*). However, we noticed that *RUNX3/AML2* was confined mostly to the lymphoid lineage and was relatively high in NK92 cells. *RUNX3* is closely related to two other runt family members, *RUNX1* and *RUNX2*. We focused on *RUNX1* and *RUNX3*, quantitatively confirming their expression by real-time PCR. The results mirrored the semiquantitative RT-PCR results for the most part (Fig. 3*C*). Human cell lines express varying amounts of *RUNX1* when compared with NK92. *RUNX3* was highest in NK92 and IM-9, whereas other cell lines expressed undetectable levels or levels more than 5-fold less when compared with NK92.

Using semiquantitative RT-PCR, we also checked *Runx1* and *Runx3* mRNA in mouse NK cell lines, LNK and KY-2, as well as non-NK cell lines, NIH-3T3 and Ms1. In the mouse NK cell lines, *Ncr1* and *Runx3* are detectable, whereas in the non-NK cell lines, only *Runx1* is detectable (supplemental Fig. S3). These human and mouse results agree with primary tissue data from publicly available microarray studies (Fig. 3*D*, supplemental Fig. S3).

Next, we aligned ~400 bp upstream of *NCR1* from 10 mammalian species using European Bioinformatics Institute (EBI) ClustalW2 and checked whether the binding motifs identified by TESS were conserved (Fig. 3*A*, supplemental Fig. S1). This alignment revealed that only two RUNX sites and one ETS site were highly conserved. The enhancing region harbors one RUNX site that matches the RUNX consensus (ACCACA). The essential region contains an imperfect binding site (ACCACT) and an ETS site. Both the expression data and the binding motif conservation at *NCR1* promoter point toward RUNX proteins as possible regulators of *NCR1*.

Human and Mouse NK Cells Use Distal Promoter of RUNX3—The presence of *RUNX3* transcripts does not guarantee functional RUNX3 protein. In both human and mouse, expression of *RUNX3* is regulated by two promoters (26, 27). Although *Runx3* mRNA can be detected in both mouse CD8+ and CD4+ T cells, only the CD8+ population expresses the distal transcript isoform and detectable levels of RUNX3 protein (28, 29). In mouse NK cells, the distal form of *Runx3* transcript is expressed starting at the CD122+ NK1.1−, NKP stage. RUNX protein has also been found in mouse NK lysates using a pan-RUNX antibody (30).

The transcription factor screen in Fig. 3, *B* and *C*, utilized primers that did not differentiate between proximal and distal *RUNX3*. To resolve this issue, we performed RT-PCR using promoter-specific primers. In NK92 cells, the distal transcript was preferentially expressed, and the proximal transcript was barely detectable (Fig. 4*B*). By Western blotting, RUNX3 protein can be seen in NK92 nuclear extracts (Fig. 4*C*). Therefore,

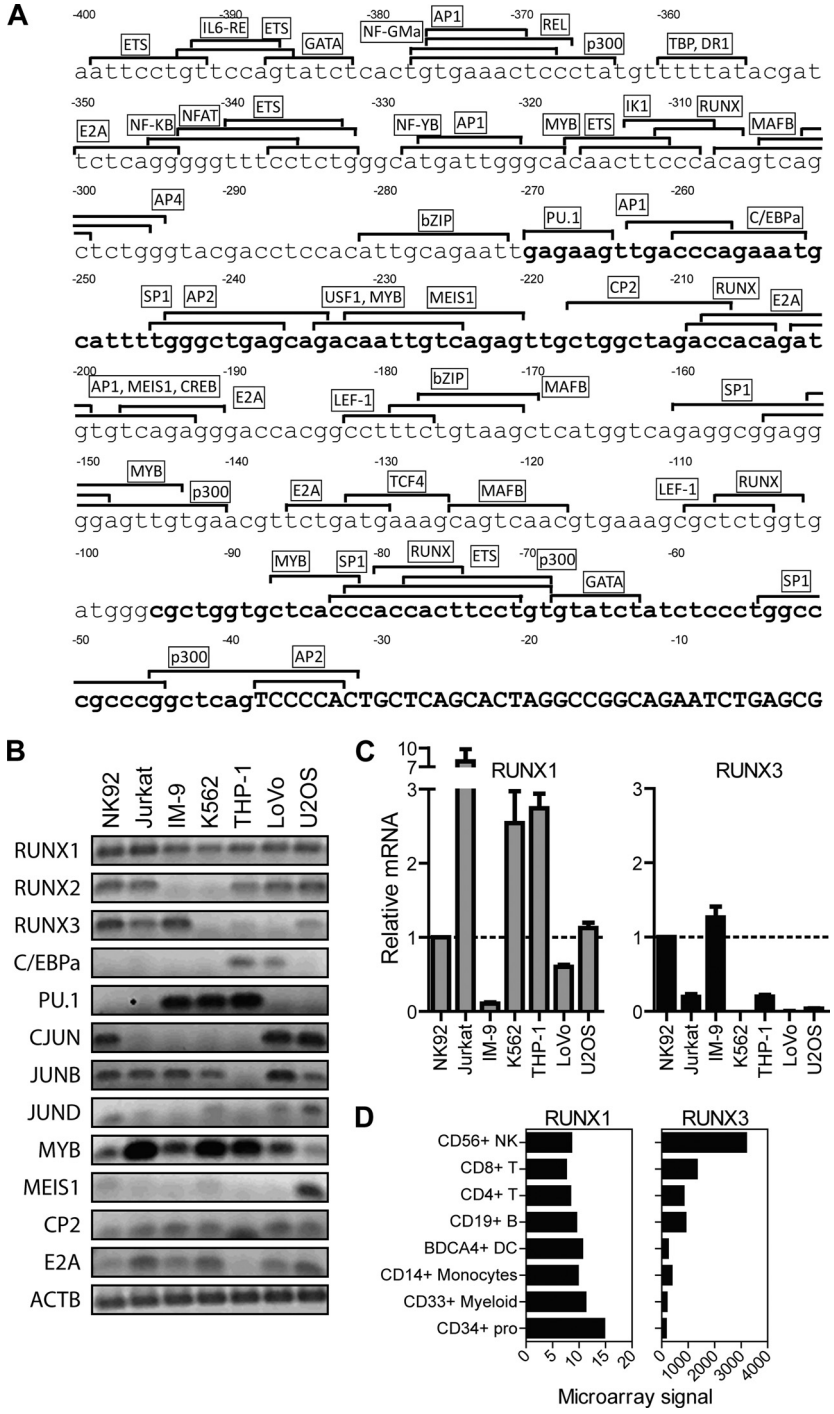

FIGURE 3. **Identification of RUNX sites in *NCR1* promoter.** *A*, TESS search for transcription factor binding sites in the *NCR1* promoter. Potential binding motifs are indicated in *brackets*. Only mammalian hematopoietic related factors are shown. *Lowercase* and *uppercase* denote intergenic and genic sequences, respectively. Sequences in *bold* indicate the enhancing and essential regions. *TBP*, TATA-binding protein; *NFAT*, nuclear factor of activated T-cells; *CREB*, cAMP-response element-binding protein; *C/EBPa*, CCAAT-enhancer-binding protein α. *B*, RT-PCR detection of transcription factors in human cell lines. Total RNA from indicated cell lines was used for reverse transcriptase reactions. Primers as indicated under "Experimental Procedures" were used to detect various transcription factors and *ACTB*. *C*, real-time PCR detection of *RUNX1* and *RUNX3*. Transcript levels of the two *RUNX* members were assayed and normalized to *ACTB*. mRNA levels in the NK92 cell line were set to one. Data shown represent means with standard deviations of three experiments. *D*, microarray of *RUNX3* expression. Data accessed through BioGPS (51) from GeneAtlas U133A probe set 207860_at (52). Only relevant hematopoietic cell types are shown.

human NK cells express the distal form of RUNX3 at the mRNA and protein levels.

RUNX Binding Motif Mutations Decrease NCR1 Promoter Strength—The essential and enhancing regions contain a well conserved RUNX binding site each. We hypothesized that the recognition motifs were important to *NCR1* promoter activity. Mutations were introduced to these motifs in our pGL4B construct containing the promoter from +1 to −270. Luciferase assays were then performed in NK92 cells. Destroying the RUNX binding site in the enhancing region results in a drop of promoter strength from 13- to 4-fold above background (Fig. 5). When the same mutation was introduced into the motif in the essential region,

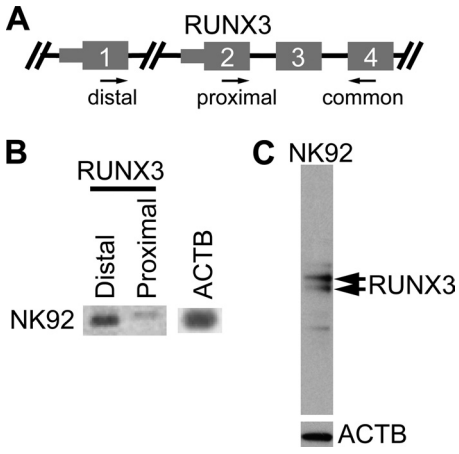

FIGURE 4. **NK cells express distal RUNX3.** *A*, diagram of *RUNX3* gene structure at the 5′ end. *Thin* and *thick gray boxes* represent 5′-UTR and coding regions, respectively. *Arrows* indicate primers used to detect *RUNX3* mRNA isoforms: distal forward, proximal forward, and common reverse primers. *B*, RT-PCR detection of *RUNX3* isoforms in human NK cell lines. Total RNA from NK92 was used for reverse transcriptase reactions. *C*, Western blot analysis of RUNX3 protein in NK92. Immunoblotting was performed on nuclear extracts. *Arrows* in the *upper panel* correspond to the positions of RUNX3 protein (using anti-human RUNX3 antibody), and the *lower panel* shows the position of ACTB protein (loading control).

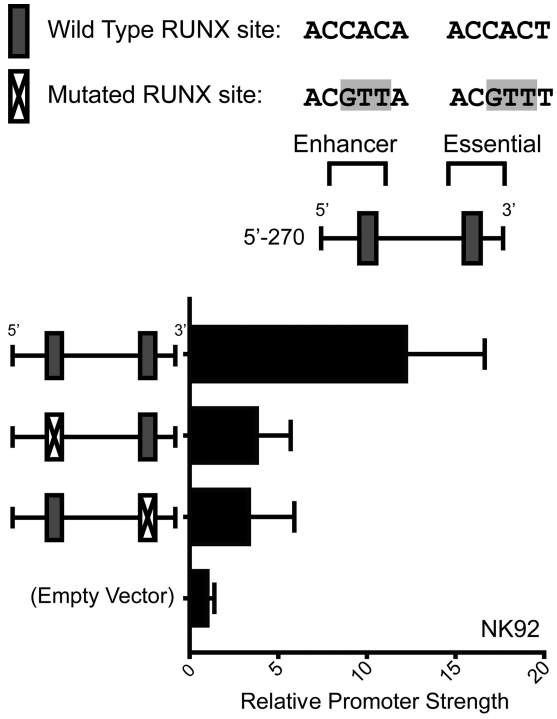

FIGURE 5. **RUNX motif mutations decrease *NCR1* promoter strength.** Mutations shown at the *top* were introduced into a promoter fragment from +1 to −270 in pGL4B backbone. The vector was transiently transfected into NK92, and luciferase activity was measured using a Dual-Luciferase system. Firefly luciferase activity was normalized to co-transfected *Renilla* luciferase and calculated as -fold above the pGL4B empty vector. Data shown represent means with standard deviations of three experiments.

promoter strength decreased to 3-fold above background. However, we cannot rule out a contribution from the ETS binding site because the mutation overlaps both the putative RUNX site and the putative ETS site. The results indicate that these motifs are required for optimal expression from the *NCR1* promoter.

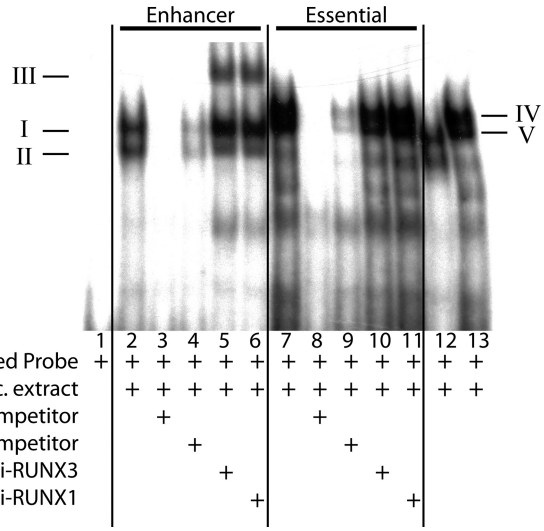

FIGURE 6. **RUNX forms protein-DNA complexes with *NCR1* promoter elements *in vitro*.** EMSA was performed using probes containing RUNX motifs in the enhancer (*lanes 2–6*) and essential (*lanes 7–11*) region. A side-by-side comparison of band shift patterns between the two regions is shown in *lanes 12* and *13*. As control, *lane 1* contains only γ-^{32}P-labeled WT enhancer and essential probe. NK92 nuclear extract (*NK92 nuc. extract*) was incubated with labeled WT probe at 4 °C for 20 min (*lanes 2* and *7*). For competition assays, unlabeled competitors were incubated with NK92 nuclear extract at 4 °C for 20 min before the addition of labeled WT probe. Competitors were used at 200-fold excess (*lanes 3*, *4*, *8*, and *9*). Supershift assays were carried out using anti-RUNX3 (*lanes 5* and *10*) or anti-RUNX1 (*lanes 6* and *11*) antibodies. *I*, *II*, *IV*, and *V* represent band shifts of DNA-protein interaction. *III* represents band supershift of DNA-protein-antibody interaction.

RUNX3 and RUNX1 Bind Promoter in Vitro—All members of the runt family bind the conserved motif, 5′-ACCRCA-3′. We wondered whether either RUNX1 or RUNX3 can indeed bind the predicted motifs in the NCR1 promoter. To test this possibility, electrophoretic mobility shift assays (EMSA) were performed. We tested the two RUNX sites separately. Probes spanning the putative RUNX binding site in the enhancer were shifted by NK92 nuclear extract (Fig. 6). Two bands are clearly visible, labeled *I* and *II*. The bands were completely abolished with the introduction of unlabeled wild type competing oligomers at 200-fold excess. If unlabeled competing oligomers with a mutated RUNX site were used instead, both band I and band II were still visible, although weaker. The decrease in signal strength is likely the result of nonspecific binding of mutant probes at molar excess. We confirmed that the identities of the binding proteins were RUNX3 and RUNX1 by supershift experiments. When anti-RUNX3 or anti-RUNX1 was incubated with NK92 nuclear proteins beforehand, a supershifted band III was observed. Band II, whose signal strength decreased, most likely contains the RUNX3/RUNX1-DNA complexes. The identity of band I is currently unknown.

Probes spanning the predicted RUNX binding site in the essential region were also shifted by NK92 nuclear extract (Fig. 6). Again, multiple bands are visible, labeled *IV* and *V*. The bands completely disappear with competition from wild type but not mutant unlabeled oligomers at 200-fold excess. Neither anti-RUNX3 nor anti-RUNX1 antibodies supershifted these bands. Thus, the nuclear proteins binding the essential region and forming bands IV and V are neither RUNX1 nor RUNX3. Side-by-side comparison of shift patterns between the essential

and enhancer regions show that the band positions are not the same, further hinting that RUNX proteins are not binding the essential region. The most likely candidates remaining are ETS family members, based on our motif prediction and reporter assay results. Taken together, these results suggest that RUNX1 and RUNX3 both bind the enhancer region in the *NCR1* promoter.

RUNX3 and RUNX1 Bind Promoter in Vivo—In vitro binding of transcription factors to DNA is not always reflective of *in vivo* states due to the variability of chromatin context. We therefore examined whether RUNX1 and RUNX3 were enriched at the human *NCR1* promoter specifically in NK cells by using chromatin immunoprecipitation (ChIP). As a negative control, we chose an intergenic region 8 kb downstream of *NCR1*. This region is not known to contain any regulatory sequences. As a positive control, we analyzed the promoter of *CD122*. We chose this because in mouse NK cells, the *Cd122* promoter was previously shown to bind RUNX protein using a pan-RUNX antibody (30). We performed the ChIP assay using anti-human RUNX3- and anti-human RUNX1-specific antibodies. In NK92 cells, the negative control region did not show significant enrichment of either transcription factor (Fig. 7*A*). The *CD122* promoter shows significant enrichment of RUNX1 (7-fold) and RUNX3 (11-fold) over isotype background. At the *NCR1* promoter, we also detected significant enrichment of RUNX1 (5-fold) and RUNX3 (16-fold).

To determine whether RUNX binding to the *NCR1* promoter is NK-specific, ChIP was performed in other cell lines. We chose IM-9 and U2OS. When compared with NK92, IM-9 expresses equivalent levels of *RUNX3* transcripts, but 10-fold less *RUNX1*. On the other hand, U2OS expresses equivalent levels of *RUNX1* transcripts, but 25-fold less *RUNX3* (Fig. 3*C*). Neither of these cells showed enrichment for RUNX1 or RUNX3 at *NCR1* promoter (Fig. 7*A*). Thus, RUNX transcription factors bind *NCR1* promoter in an NK-specific manner.

In a *Runx3*-deficient mouse, flow cytometric analysis revealed that NKp46 is expressed at a level comparable with wild type.[3] We wondered whether Runx1 can compensate for Runx3 in regulating *Ncr1* expression. To test this possibility, we performed ChIP on NK cells isolated from *Runx3* knock-out and wild type mice. In wild type NK cells, we could not detect Runx1 enrichment at the *Ncr1* promoter when compared with isotype levels. However in *Runx3*-deficient NK cells, RUNX1 is enriched at the same location by about 3-fold (Fig. 7*B*). These results indicate that in mouse NK cells, RUNX1 does not bind *Ncr1* promoter normally but takes the place of RUNX3 when the latter is absent.

Dominant Negative RUNX Interferes with NCR1 Transcription—To test the effects of all RUNX proteins on *NCR1* expression, we used mouse dn-RUNX (30). dn-RUNX consists of the DNA binding Runt domain of RUNX transcription factors, without the transactivation domain. Because all RUNX members bind the same motif, dn-RUNX acts as a pan-RUNX competitive inhibitor. We retrovirally introduced dn-RUNX into KY-2 and isolated successful transductants at two

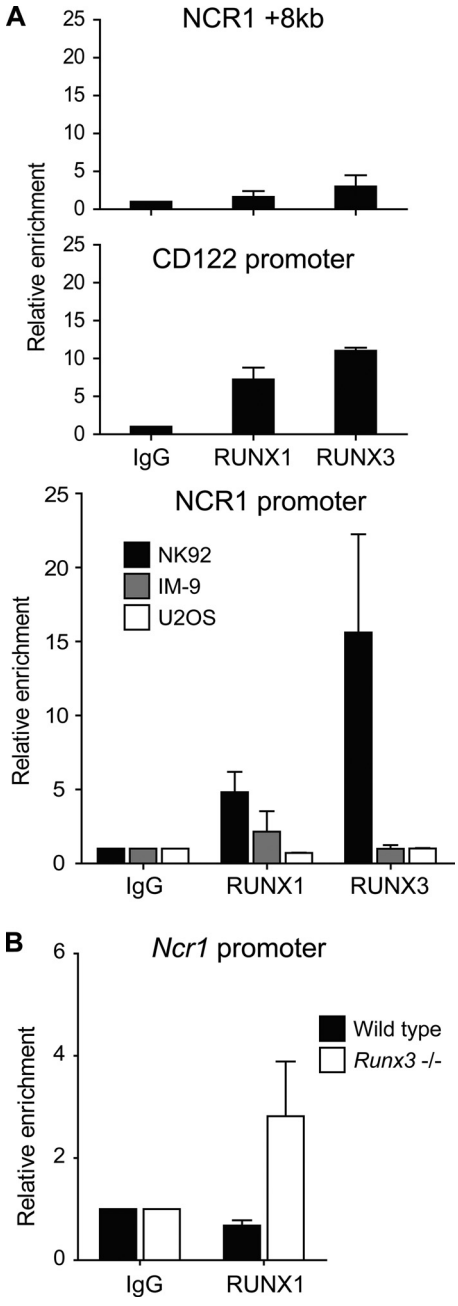

FIGURE 7. **RUNX binds *NCR1* promoter *in vivo*.** ChIP was performed in NK92, IM-9, and U2OS (*A*) and mouse wild type and *Runx3*-deficient NK cells (*B*) using anti-human RUNX3, anti-human/mouse RUNX1, and IgG isotype control. Precipitated DNA was assayed by real-time PCR using primers specific for the human *NCR1* promoter, an intergenic region 8 kb downstream of human *NCR1*, the human *CD122* promoter, and the mouse *Ncr1* promoter. Enrichment is calculated as -fold over IgG control. Data shown represent means with standard deviations of three experiments.

time points, days 4 and 6 after transduction. The isolation was achieved by fluorescence-activated cell sorting (FACS) using the GFP marker on the vector. Transcript levels of various genes were assayed by real-time PCR.

18S RNA, which acts as a negative control, did not change significantly throughout the time points (Fig. 8). As positive controls, we looked at *Ifng*, *Prf1* (perforin 1), and *Cd43* (sialophorin). Interferon γ and perforin have been shown to be regulated by *Runx3* in mouse CD4+ and CD8+ T cells (31–34).

[3] D. Levanon, personal communication.

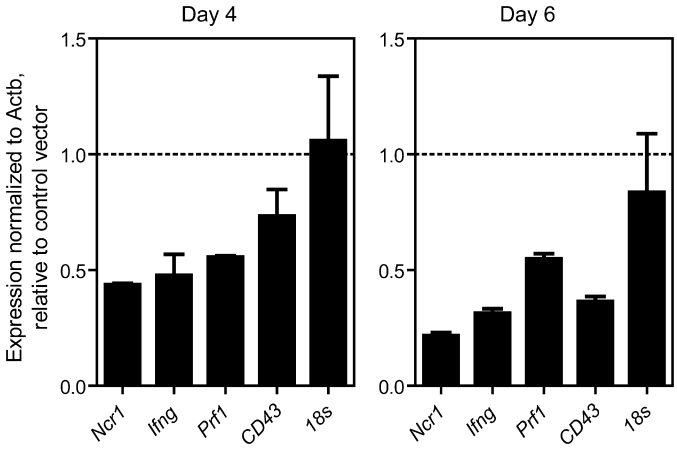

FIGURE 8. **dn-RUNX decreases *Ncr1* expression.** Gene expression was measured by real-time PCR. *Actb* is the endogenous control. Expression levels in dn-RUNX transductants were normalized to levels in empty vector control transductants. Data shown represent means with standard deviations of three experiments.

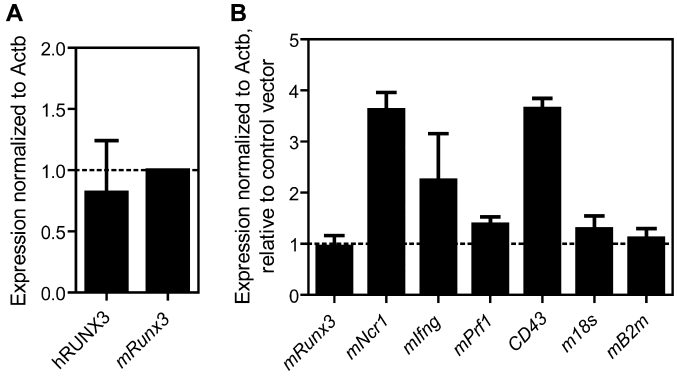

FIGURE 9. **RUNX3 overexpression enhances *Ncr1* expression.** Gene expression was measured by real-time PCR with *Actb* as the endogenous control. *A*, expression of human *RUNX3* levels in MIY-hRUNX3 transductants with respect to endogenous mouse *Runx3* (*mRunx3*, set to 1). *B*, expression of various genes in these transductants normalized to levels in empty vector control transductants. Data shown represent means with standard deviations of three experiments.

Additionally, Ohno *et al.* (30) showed that interferon γ and CD43 are perturbed in dn-RUNX-expressing NK cells. When compared with empty vector-transduced KY-2 cells, dn-RUNX-transduced cells show decreased expression of all positive control genes to ~50% for *Ifng* and *Prf1* and 73% for CD43 on day 4. On day 6, the down-regulation of these genes was more pronounced, ranging from 17 to 55% expression when compared with empty vector control. *Ncr1* was similarly decreased in expression at both time points (44 and 22% on days 4 and 6 when compared with empty vector, respectively). These results suggest that the RUNX proteins are required for optimal transcription of *Ncr1*, differentiation markers, and effector genes in mouse NK cells.

RUNX3 Overexpression Increases NCR1 Expression—To more directly examine the role of RUNX3 in regulation of *NCR1*, we decided to overexpress RUNX3 in NK cells. We transduced human *RUNX3* (*hRUNX3*) cDNA into KY-2 cells and selected using the vector YFP by FACS. Human *RUNX3* expression in mouse KY-2 was verified by real-time PCR (Fig. 9*A*). Overexpression of *hRUNX3* did not lead to an increase in endogenous mouse *Runx3*, nor the negative controls, *18S* RNA and β-2 microglobulin (Fig. 9*B*). Interestingly, *Prf1* mRNA levels did not change. Additionally, although *Ifng* levels seemed to increase mildly, the change was not statistically significant. Both *Cd43* and *Ncr1* mRNA increased almost 4-fold when compared with empty vector control. These results imply that RUNX3 specifically contributes to *Cd43* and *Ncr1* expression, whereas other RUNX family members may be more important in regulating *Prf1* and *Ifng*.

Promoter Behaves Differently in Non-NK Cells—We wondered whether the essential and enhancer elements of the *NCR1* promoter were tissue-specific. Thus, we ran luciferase assays using the 5′ truncation constructs in the U2OS cell line. In these cells, the constructs behaved differently when compared with the NK92 cells (Fig. 10*A*). The essential region by itself still confers high promoter activity, but the region between −200 and −270 actually down-regulates promoter strength. This trend is also observed in HeLa cells (data not shown), suggesting that the effects are not an artifact of the U2OS cell line. Thus, the essential region acts primarily as a pan-tissue promoter. On the other hand, the −200 to −270 region acts as an enhancer or suppressor, depending on the cellular context (henceforth termed the switch region).

Furthermore, we investigated the chromatin context of the promoter in NK92 and IM-9 cells. To this end, we performed ChIP using antibodies toward histone modifications histone 3 lysine 4 trimethylation (H3K4me3) and histone 3 lysine 27 trimethylation (H3K27me3). H3K4me3 is a chromatin mark strongly linked to the promoters of actively transcribing genes, whereas the H3K27me3 mark is considered repressive and linked to silent loci (35). H3K4me3 was found to be highly enriched at the NCR1 promoter only in NK92 cells (Fig. 10*B*). Conversely, at the same location, IM-9 cells display preferential enrichment of H3K27me3. Thus, the chromatin configuration is favorable to expression in NK cells and closed in non-NK cells.

DISCUSSION

Tissue-restricted expression is not an uncommon phenomenon. What makes *NCR1* unique is the small number of known NK-specific genes. Even more remarkable is the fact that the specificity can arise from a short proximal promoter of ~270 bp. The luciferase assay results further show the lineage-limiting sequence to be confined to a 70-bp region.

Within the switch region, we found a runt binding motif. The binding motif is the same for all members of the runt family: RUNX1, RUNX2, and RUNX3. RUNX1 is a crucial transcription factor in the hematopoietic system. Its deficiency results in blocked hematopoiesis during development, and conditional mutants have abnormalities in lymphoid as well as myeloid lineages (36). The transcription factor is also known to regulate multiple hematopoietic genes (37). RUNX2 is primarily involved in bone formation and not so much in hematopoiesis (37). Finally, RUNX3 is a key player in T cell development and function. *Runx3* knock-out models indicate that the protein is required for cytotoxic T lymphocyte specification, down-regulating CD4, and up-regulating CD8 (38, 39). RUNX3 is re-expressed when naive CD4 T cells differentiate into TH1 but not TH2 cells (31). In CD8 T cells and TH1 cells, RUNX3 controls

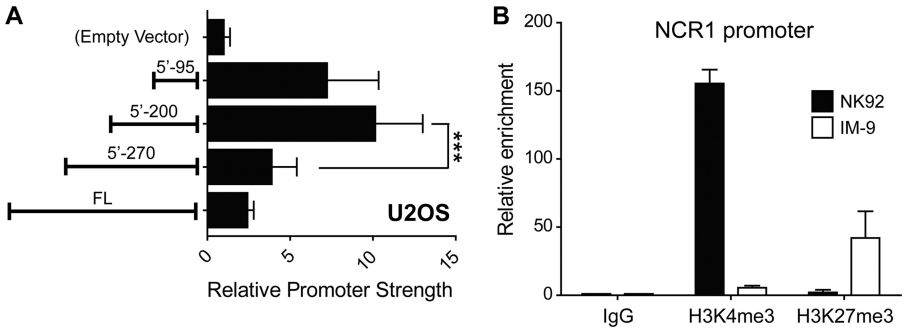

FIGURE 10. **NCR1 promoter in non-NK cells.** *A*, 5′ truncation promoter constructs as in Fig. 2 were transiently transfected into U2OS cells. Firefly luciferase activity was assayed normalized to co-transfected *Renilla* luciferase activity. Promoter strength is calculated as -fold above pGL4B empty vector. Data shown represent means with standard deviations of more than three experiments. Tests of significance were carried out using analysis of variance followed by Tukey's post test (***, $p < 0.001$). *B*, ChIP was performed in NK92 and IM-9 cells using anti-human H3K4me3, anti-human H3K27me3, and IgG isotype control. Precipitated DNA was assayed by real-time PCR using primers specific for the *NCR1* promoter. Enrichment is calculated as -fold over IgG control. Data shown represent means with standard deviations of three experiments.

multiple effector function genes including granzyme, interferon γ, and perforin. Indeed, the current paradigm indicates both RUNX1 and RUNX3 to be important players in T cell differentiation (37, 40).

In NK cells, the importance of the RUNX proteins is only beginning to emerge. The human killer immunoglobulin-like receptor (KIR) genes are known to have RUNX binding sites, and variants with mutated RUNX sites are not expressed (41). The cofactor for the RUNX proteins, core binding factor β (Cbfβ), is required for proper mouse NK cell development (42). Furthermore, *Runx* proteins regulate genes such as *Cd122* and *Ly49*, and *Runx3* undergoes a dramatic up-regulation during NK differentiation; it is low in hematopoietic stem cells and peaks at the immature NK stage (30, 42). Certainly, when comparing different hematopoietic cell types, *RUNX3* seems to be consistently overexpressed in NK cells in human and mouse. In our cell lines, only IM-9 matched the high level of *RUNX3* expression in NK cells. It is known that naive B cells usually express *RUNX1*, but switch to *RUNX3* when transformed by Epstein-Barr virus (43). This could explain why IM-9, an Epstein-Barr virus-transformed B lymphoblastic cell line, has *RUNX3* mRNA levels as high as NK92 cells. We link RUNX1 and RUNX3 directly to an important determinant of NK function by showing that these transcription factors bind a RUNX site in the endogenous *NCR1* promoter. A pan-RUNX dominant negative protein disrupts optimal *NCR1* expression, whereas *RUNX3* overexpression has the opposite effect. Although both RUNX1 and RUNX3 can bind the enhancer region, the higher level of *RUNX3* expression in NK cells may result in preferred binding of RUNX3 at the *NCR1* promoter. We hypothesize that RUNX1 may act as a redundant factor and bind the promoter if RUNX3 is disrupted. This redundancy is not surprising if one takes into account the relative importance of the NCR1 receptor in host immune defense.

Our dn-RUNX results also show a down-regulation of *Ifng* and *Prf1*, indicating a link between the RUNX proteins and NK effector function. In contrast, Ohno *et al.* (30) showed that dn-RUNX up-regulated *Ifng*. This discrepancy may be due to several fundamental differences in methodology. Ohno *et al.* (30) used NK1.1+CD3− cells from spleen of dn-RUNX transgenic mice to test intracellular IFNG protein levels. We used a dn-RUNX-transduced mouse NK cell line and tested transcript levels by real-time PCR. It is also possible that RUNX affects *Ifng* differently at transcriptional and translational levels.

Already, the limited amount of evidence available for RUNX3 in NK, CD8+ T, and TH1 cells implicates the transcription factor as an important mediator of cell-mediated immunity. Of course, this notion suggests that RUNX3 alone is not enough to direct NK specificity, instead merely potentiates transcription in cytotoxic and TH1 lymphocytes. In fact, no single transcription factor has been shown to conclusively act as a "master regulator" of the NK program so far. Such a factor would be required for the expression of the NK program and repression of non-NK genes. Another possibility is that multiple factors that are not lineage-specific act in a combinatorial way to restrict expression of NK genes such as *NCR1*. RUNX3 could be such a factor, and the search is still on to identify others.

To date, no studies have investigated the NK compartment in the existing complete *Runx3* knock-out mouse models (44). With the development of the *Ncr1-cre* mouse, it is now possible to delete genes specifically in the NK lineage. Although *Ncr1* is under the control of *Runx3*, it should still be possible to selectively delete the *Runx3* locus. Studies that examine the downstream targets of RUNX3 could lead to new perspectives in NK cell biology.

The pathway leading to *RUNX3* expression is also of interest. Park *et al.* (45) recently showed that RUNX3 is induced by common γ chain (γc) receptor signaling during CD8 T specification. The process is dependent on STAT5 or STAT6 as γc-related cytokine stimulation of thymocytes from *Stat5/6* double knock-out mouse did not induce *Runx3* expression. Major γc receptors are also known to play important roles in NK development and stimulation (46). Downstream of the receptors, *Stat5* deficiency in NK was recently shown to lead to a blockage at the Lin-CD122+ NKP stage (17). Finally, RUNX proteins positively regulate interleukin-2 receptor β (IL2Rβ)/CD122 in NK cells (30). The link between STAT5/6 and RUNX3 in NK cells still needs to be experimentally established. However, the emerging picture is one where the IL-15 receptor, which first appears in the NKP stage, activates the appropriate STAT members including STAT5 in cells committed to the NK lineage. This axis may lead to induction of transcription factors including RUNX3 to turn on NK-related genes such as *NCR1*. RUNX3, in turn, acts in a positive feedback loop to further

up-regulate IL2Rβ/CD122, a subunit of the IL-15 receptor. In fact, surface NKp46 can be forcibly induced in a small proportion of human CD8+ T cells (~5%), when these cells are cultured *ex vivo* for 12 days with IL-15 (47). This suggests that the axis plays an important, although by itself not sufficient, role in the NK program.

Aside from the runt binding motif, we also noticed an ETS binding motif that can contribute to *NCR1* transcriptional regulation. The ETS family transcription factors have many members, and a few in particular are known to participate in NK development and function (48). Furthermore, we previously showed that GA-binding protein (GABP), another member of the family, is required for optimal although not absolute expression of the mouse *Nkg2d* long isoform (49). The ETS motif in the *NCR1* promoter lies in the essential region, which does not seem to be responsible for tissue specificity. Nevertheless, mutations to the binding site affect the activity of the promoter. Although an imperfect RUNX binding site was identified right next to the ETS site, we could not detect binding of RUNX1 nor RUNX3 to this site *in vitro*. Thus, these RUNX proteins seem to be solely involved in enhancing promoter activity in the NK lineage, whereas ETS proteins may be involved in setting up the basal activity.

In non-NK cells, we observed that the essential region by itself has appreciable promoter activity. However, this activity is suppressed by the switch region. The flip of function in this cis-regulatory region is intriguing as it suggests that NK specificity requires a dual mode of control: context-dependent enhancer and repressor. The identity of the suppressing transcription factor remains a mystery. The RUNX proteins do possess repressor activity depending on bound co-repressors or histone deacetylases (50). However, they are not bound to the *NCR1* promoter in non-NK cells and thus are unlikely to be involved in repression of *NCR1* expression. Histone modifications act as an additional level of tissue-specific control because we found the enrichment of permissive and repressive chromatin marks in NK and non-NK cell lines, respectively.

An understanding of *NCR1* regulation bears clinical as well as research potential. Because mouse models show a strong relationship between the receptor and diseases such as influenza and diabetes, one clinical goal is to efficaciously manage the expression of the receptor to benefit disease outcomes. Such studies also provide insight into the understanding of the NK program, which noticeably lags behind our understanding of T and B lymphocyte programs. As the usage of the *NCR1* promoter for transgenic studies gains traction, rational manipulation of the promoter will provide greater flexibility in the usage of this great tool.

Acknowledgments—We thank Dr. Ditsa Levanon and Varda Negreanu for sharing Runx3 knock-out mouse NK cells as well as valuable discussion and advice. The RUNX dominant negative and RUNX3 overexpression retrovirus constructs were kind gifts from Dr. Takehito Sato and Dr. Aly Karsan. We are grateful for technical help and discussions from Dr. Ping Xiang, Samuel Gusscott, Christopher Jenkins, and Rebecca Cullum. We also thank the Terry Fox Laboratory FACS facility staff for cell sorting.

REFERENCES

1. Vivier, E., Tomasello, E., Baratin, M., Walzer, T., and Ugolini, S. (2008) Functions of natural killer cells. *Nat. Immunol.* **9,** 503–510
2. Paust, S., and von Andrian, U. H. (2011) Natural killer cell memory. *Nat. Immunol.* **12,** 500–508
3. Colucci, F., Di Santo, J. P., and Leibson, P. J. (2002) Natural killer cell activation in mice and men: different triggers for similar weapons? *Nat. Immunol.* **3,** 807–813
4. Sivori, S., Vitale, M., Morelli, L., Sanseverino, L., Augugliaro, R., Bottino, C., Moretta, L., and Moretta, A. (1997) p46, a novel natural killer cell-specific surface molecule that mediates cell activation. *J. Exp. Med.* **186,** 1129–1136
5. Mandelboim, O., Lieberman, N., Lev, M., Paul, L., Arnon, T. I., Bushkin, Y., Davis, D. M., Strominger, J. L., Yewdell, J. W., and Porgador, A. (2001) Recognition of hemagglutinins on virus-infected cells by NKp46 activates lysis by human NK cells. *Nature* **409,** 1055–1060
6. Elboim, M., Gazit, R., Gur, C., Ghadially, H., Betser-Cohen, G., and Mandelboim, O. (2010) Tumor immunoediting by NKp46. *J. Immunol.* **184,** 5637–5644
7. Gazit, R., Gruda, R., Elboim, M., Arnon, T. I., Katz, G., Achdout, H., Hanna, J., Qimron, U., Landau, G., Greenbaum, E., Zakay-Rones, Z., Porgador, A., and Mandelboim, O. (2006) Lethal influenza infection in the absence of the natural killer cell receptor gene Ncr1. *Nat. Immunol.* **7,** 517–523
8. Halfteck, G. G., Elboim, M., Gur, C., Achdout, H., Ghadially, H., and Mandelboim, O. (2009) Enhanced *in vivo* growth of lymphoma tumors in the absence of the NK-activating receptor NKp46/NCR1. *J. Immunol.* **182,** 2221–2230
9. Gur, C., Porgador, A., Elboim, M., Gazit, R., Mizrahi, S., Stern-Ginossar, N., Achdout, H., Ghadially, H., Dor, Y., Nir, T., Doviner, V., Hershkovitz, O., Mendelson, M., Naparstek, Y., and Mandelboim, O. (2010) The activating receptor NKp46 is essential for the development of type 1 diabetes. *Nat. Immunol.* **11,** 121–128
10. Kelley, J., Walter, L., and Trowsdale, J. (2005) Comparative genomics of natural killer cell receptor gene clusters. *Plos. Genet.* **1,** 129–139
11. Storset, A. K., Kulberg, S., Berg, I., Boysen, P., Hope, J. C., and Dissen, E. (2004) NKp46 defines a subset of bovine leukocytes with natural killer cell characteristics. *Eur. J. Immunol.* **34,** 669–676
12. Jozaki, K., Shinkai, H., Morozumi, T., Tanaka-Matsuda, M., Eguchi-Ogawa, T., Wada, Y., and Uenishi, H. (2010) Cloning, expression, and polymorphisms of natural killer cell receptor NCR1 in pigs. *Anim. Biotechnol.* **21,** 156–163
13. Bottino, C., Biassoni, R., Millo, R., Moretta, L., and Moretta, A. (2000) The human natural cytotoxicity receptors (NCR) that induce HLA class I-independent NK cell triggering. *Hum. Immunol.* **61,** 1–6
14. Satoh-Takayama, N., Vosshenrich, C. A., Lesjean-Pottier, S., Sawa, S., Lochner, M., Rattis, F., Mention, J. J., Thiam, K., Cerf-Bensussan, N., Mandelboim, O., Eberl, G., and Di Santo, J. P. (2008) Microbial flora drives interleukin 22 production in intestinal NKp46+ cells that provide innate mucosal immune defense. *Immunity* **29,** 958–970
15. Crellin, N. K., Trifari, S., Kaplan, C. D., Cupedo, T., and Spits, H. (2010) Human NKp44+IL-22+ cells and LTi-like cells constitute a stable RORC+ lineage distinct from conventional natural killer cells. *J. Exp. Med.* **207,** 281–290
16. Walzer, T., Bléry, M., Chaix, J., Fuseri, N., Chasson, L., Robbins, S. H., Jaeger, S., André, P., Gauthier, L., Daniel, L., Chemin, K., Morel, Y., Dalod, M., Imbert, J., Pierres, M., Moretta, A., Romagné, F., and Vivier, E. (2007) Identification, activation, and selective *in vivo* ablation of mouse NK cells via NKp46. *Proc. Natl. Acad. Sci. U.S.A.* **104,** 3384–3389
17. Eckelhart, E., Warsch, W., Zebedin, E., Simma, O., Stoiber, D., Kolbe, T., Rülicke, T., Mueller, M., Casanova, E., and Sexl, V. (2011) A novel Ncr1-Cre mouse reveals the essential role of STAT5 for NK cell survival and development. *Blood* **117,** 1565–1573
18. Gong, J. H., Maki, G., and Klingemann, H. G. (1994) Characterization of a human cell line (NK-92) with phenotypical and functional characteristics of activated natural killer cells. *Leukemia* **8,** 652–658
19. Levanon, D., Bettoun, D., Harris-Cerruti, C., Woolf, E., Negreanu, V., Eilam, R., Bernstein, Y., Goldenberg, D., Xiao, C., Fliegauf, M., Kremer, E.,

Otto, F., Brenner, O., Lev-Tov, A., and Groner, Y. (2002) The Runx3 transcription factor regulates development and survival of TrkC dorsal root ganglia neurons. *EMBO J.* **21,** 3454–3463
20. Maksakova, I. A., and Mager, D. L. (2005) Transcriptional regulation of early transposon elements, an active family of mouse long terminal repeat retrotransposons. *J. Virol.* **79,** 13865–13874
21. Wederell, E. D., Bilenky, M., Cullum, R., Thiessen, N., Dagpinar, M., Delaney, A., Varhol, R., Zhao, Y., Zeng, T., Bernier, B., Ingham, M., Hirst, M., Robertson, G., Marra, M. A., Jones, S., and Hoodless, P. A. (2008) Global analysis of *in vivo* Foxa2 binding sites in mouse adult liver using massively parallel sequencing. *Nucleic Acids Res.* **36,** 4549–4564
22. Hayashi, K., Natsume, W., Watanabe, T., Abe, N., Iwai, N., Okada, H., Ito, Y., Asano, M., Iwakura, Y., Habu, S., Takahama, Y., and Satake, M. (2000) Diminution of the AML1 transcription factor function causes differential effects on the fates of CD4 and CD8 single-positive T cells. *J. Immunol.* **165,** 6816–6824
23. Fu, Y., Chang, A. C., Fournier, M., Chang, L., Niessen, K., and Karsan, A. (2011) RUNX3 maintains the mesenchymal phenotype after termination of the Notch signal. *J. Biol. Chem.* **286,** 11803–11813
24. Morita, S., Kojima, T., and Kitamura, T. (2000) Plat-E: an efficient and stable system for transient packaging of retroviruses. *Gene Ther.* **7,** 1063–1066
25. Pessino, A., Sivori, S., Bottino, C., Malaspina, A., Morelli, L., Moretta, L., Biassoni, R., and Moretta, A. (1998) Molecular cloning of NKp46: a novel member of the immunoglobulin superfamily involved in triggering of natural cytotoxicity. *J. Exp. Med.* **188,** 953–960
26. Rini, D., and Calabi, F. (2001) Identification and comparative analysis of a second runx3 promoter. *Gene* **273,** 13–22
27. Bangsow, C., Rubins, N., Glusman, G., Bernstein, Y., Negreanu, V., Goldenberg, D., Lotem, J., Ben-Asher, E., Lancet, D., Levanon, D., and Groner, Y. (2001) The RUNX3 gene: sequence, structure, and regulated expression. *Gene* **279,** 221–232
28. Sato, T., Ohno, S., Hayashi, T., Sato, C., Kohu, K., Satake, M., and Habu, S. (2005) Dual functions of Runx proteins for reactivating CD8 and silencing CD4 at the commitment process into CD8 thymocytes. *Immunity* **22,** 317–328
29. Egawa, T., Tillman, R. E., Naoe, Y., Taniuchi, I., and Littman, D. R. (2007) The role of the Runx transcription factors in thymocyte differentiation and in homeostasis of naive T cells. *J. Exp. Med.* **204,** 1945–1957
30. Ohno, S., Sato, T., Kohu, K., Takeda, K., Okumura, K., Satake, M., and Habu, S. (2008) Runx proteins are involved in regulation of CD122, Ly49 family, and IFN-γ expression during NK cell differentiation. *Int. Immunol.* **20,** 71–79
31. Djuretic, I. M., Levanon, D., Negreanu, V., Groner, Y., Rao, A., and Ansel, K. M. (2007) Transcription factors T-bet and Runx3 cooperate to activate Ifng and silence Il4 in T helper type 1 cells. *Nat. Immunol.* **8,** 145–153
32. Wang, L., Wildt, K. F., Castro, E., Xiong, Y., Feigenbaum, L., Tessarollo, L., and Bosselut, R. (2008) The zinc finger transcription factor Zbtb7b represses CD8 lineage gene expression in peripheral CD4+ T cells. *Immunity* **29,** 876–887
33. Yagi, R., Junttila, I. S., Wei, G., Urban, J. F., Jr, Zhao, K., Paul, W. E., and Zhu, J. (2010) The transcription factor GATA3 actively represses RUNX3 protein-regulated production of interferon-γ. *Immunity* **32,** 507–517
34. Cruz-Guilloty, F., Pipkin, M. E., Djuretic, I. M., Levanon, D., Lotem, J., Lichtenheld, M. G., Groner, Y., and Rao, A. (2009) Runx3 and T-box proteins cooperate to establish the transcriptional program of effector CTLs. *J. Exp. Med.* **206,** 51–59
35. Barski, A., Cuddapah, S., Cui, K., Roh, T. Y., Schones, D. E., Wang, Z., Wei, G., Chepelev, I., and Zhao, K. (2007) High-resolution profiling of histone methylations in the human genome. *Cell* **129,** 823–837
36. Growney, J. D., Shigematsu, H., Li, Z., Lee, B. H., Adelsperger, J., Rowan, R., Curley, D. P., Kutok, J. L., Akashi, K., Williams, I. R., Speck, N. A., and Gilliland, D. G. (2005) Loss of Runx1 perturbs adult hematopoiesis and is associated with a myeloproliferative phenotype. *Blood* **106,** 494–504
37. Cohen, M. M., Jr. (2009) Perspectives on RUNX genes: an update. *Am. J. Med. Genet. A.* **149A**, 2629–2646
38. Taniuchi, I., Osato, M., Egawa, T., Sunshine, M. J., Bae, S. C., Komori, T., Ito, Y., and Littman, D. R. (2002) Differential requirements for Runx proteins in CD4 repression and epigenetic silencing during T lymphocyte development. *Cell* **111,** 621–633
39. Woolf, E., Xiao, C., Fainaru, O., Lotem, J., Rosen, D., Negreanu, V., Bernstein, Y., Goldenberg, D., Brenner, O., Berke, G., Levanon, D., and Groner, Y. (2003) Runx3 and Runx1 are required for CD8 T cell development during thymopoiesis. *Proc. Natl. Acad. Sci. U.S.A.* **100,** 7731–7736
40. Collins, A., Littman, D. R., and Taniuchi, I. (2009) RUNX proteins in transcription factor networks that regulate T cell lineage choice. *Nat. Rev. Immunol.* **9,** 106–115
41. Vilches, C., Gardiner, C. M., and Parham, P. (2000) Gene structure and promoter variation of expressed and nonexpressed variants of the KIR2DL5 gene. *J. Immunol.* **165,** 6416–6421
42. Guo, Y., Maillard, I., Chakraborti, S., Rothenberg, E. V., and Speck, N. A. (2008) Core binding factors are necessary for natural killer cell development and cooperate with Notch signaling during T cell specification. *Blood* **112,** 480–492
43. Spender, L. C., Cornish, G. H., Sullivan, A., and Farrell, P. J. (2002) Expression of transcription factor AML-2 (RUNX3, CBF(α)-3) is induced by Epstein-Barr virus EBNA-2 and correlates with the B cell activation phenotype. *J. Virol.* **76,** 4919–4927
44. Levanon, D., and Groner, Y. (2009) Runx3-deficient mouse strains circa 2008: resemblance and dissimilarity. *Blood Cells Mol. Dis.* **43,** 1–5
45. Park, J. H., Adoro, S., Guinter, T., Erman, B., Alag, A. S., Catalfamo, M., Kimura, M. Y., Cui, Y., Lucas, P. J., Gress, R. E., Kubo, M., Hennighausen, L., Feigenbaum, L., and Singer, A. (2010) Signaling by intrathymic cytokines, not T cell antigen receptors, specifies CD8 lineage choice and promotes the differentiation of cytotoxic lineage T cells. *Nat. Immunol.* **11,** 257–264
46. Williams, N. S., Klem, J., Puzanov, I. J., Sivakumar, P. V., Schatzle, J. D., Bennett, M., and Kumar, V. (1998) Natural killer cell differentiation: insights from knockout and transgenic mouse models and *in vitro* systems. *Immunol. Rev.* **165,** 47–61
47. Correia, M. P., Costa, A. V., Uhrberg, M., Cardoso, E. M., and Arosa, F. A. (2011) IL-15 induces CD8+ T cells to acquire functional NK receptors capable of modulating cytotoxicity and cytokine secretion. *Immunobiology* **216,** 604–612
48. Hesslein, D. G., and Lanier, L. L. (2011) Transcriptional control of natural killer cell development and function. *Adv. Immunol.* **109,** 45–85
49. Lai, C. B., Zhang, Y., Rogers, S. L., and Mager, D. L. (2009) Creation of the two isoforms of rodent NKG2D was driven by a B1 retrotransposon insertion. *Nucleic Acids Res.* **37,** 3032–3043
50. Durst, K. L., and Hiebert, S. W. (2004) Role of RUNX family members in transcriptional repression and gene silencing. *Oncogene* **23,** 4220–4224
51. Wu, C., Orozco, C., Boyer, J., Leglise, M., Goodale, J., Batalov, S., Hodge, C. L., Haase, J., Janes, J., Huss, J. W., 3rd, and Su, A. I. (2009) BioGPS: an extensible and customizable portal for querying and organizing gene annotation resources. *Genome Biol.* **10,** R130
52. Su, A. I., Wiltshire, T., Batalov, S., Lapp, H., Ching, K. A., Block, D., Zhang, J., Soden, R., Hayakawa, M., Kreiman, G., Cooke, M. P., Walker, J. R., and Hogenesch, J. B. (2004) A gene atlas of the mouse and human protein-encoding transcriptomes. *Proc. Natl. Acad. Sci. U.S.A.* **101,** 6062–6067
53. Lattin, J. E., Schroder, K., Su, A. I., Walker, J. R., Zhang, J., Wiltshire, T., Saijo, K., Glass, C. K., Hume, D. A., Kellie, S., and Sweet, M. J. (2008) Expression analysis of G Protein-Coupled Receptors in mouse macrophages. *Immunome Res.* **4,** 5